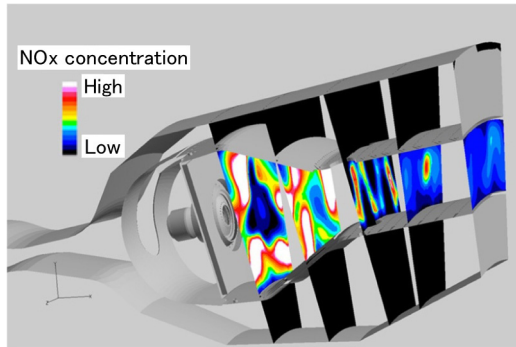


Effects of Dilution Flow Balance and Double-wall Liner on NOx Emission in Aircraft Gas Turbine Engine Combustors



HIDEKI MORIAI*¹

Environmental regulations on aircraft, including NOx emissions, have been enhanced over the past several years. Therefore, technologies for accurately predicting the amount of NOx emission from the combustor, the emission source of the aircraft gas turbine engine, are very important. In this study, the effects of the dilution flow balance between the outer and the inner liners of the combustor and the difference between the single-wall liner and the double-wall liner on NOx emission performance were predicted using computational fluid dynamics (CFD), and an experimental verification for those CFD results was performed. The results indicated that the use of CFD allows qualitative prediction of the flow inside the combustor and NOx emission performance, and that evenly balancing the dilution flow of the outer and inner liners and the use of a double-wall liner are effective for reduction of NOx.

1. Introduction

Due to increasing global environmental awareness, the control of aircraft emissions, targeting those in small quantities such as NOx, CO and particulate matter (PM), has become more stringent. The combustor, which is one of the core components of an aircraft engine and a source of such emissions, will increasingly become the focus of future aircraft engine development.

Development of combustors for aircraft engines typically takes considerable time and incurs large costs, because such development includes the process of fabricating an extensive amount of combustor hardware that complies with the required specifications using existing products and data, as well as the process of satisfying the performance specifications through trial and error, mainly through repeated experiments and design improvements. Therefore, if these processes can be substituted with numerical prediction, the time period and the cost of combustor development can be reduced considerably.

However, because the internal flow of an aircraft engine combustor consists of complicated phenomena, including turbulent mixing along with spraying, atomizing, and swirling of liquid fuel, as well as a huge number of chemical reaction mechanisms, reproduction through numerical simulation is very difficult, and even today there are few tools with sufficiently high prediction accuracy for this purpose. In recent years, Large Eddy Simulation (LES), which has a small number of adjustment parameters for modeling and can simulate unsteady turbulent flow, has attracted a great deal of attention. However, LES has not been established as a practical design tool for actual combustors, because the atomization model and turbulence combustion model for the spray combustion field of LES are still in the study phase and the calculation load of LES is very high; therefore, significant computer resources are required⁽¹⁾.

Accordingly, the main method used in current practice is Reynolds-Averaged Navier-Stokes (RANS) simulation, which obtains a steady mean field where turbulence phenomena are averaged. RANS simulation has lower accuracy than LES, but it can be used sufficiently as a design tool through proper interpretation of its results due to its reasonable computational costs.

*1 Ph. D., Engineering Manager, Engines & Control Equipment Engineering Department, Guidance & Propulsion Division, Integrated Defense & Space Systems

In this study, the internal spray combustion flow of an aircraft engine low-NO_x combustor was simulated using RANS simulation to examine its effectiveness.

In particular, we focused on the influences on NO_x emission and verification was performed with combustion test data in the case where the dilution flow balance between the outer and inner liners was changed and in the case where the outflow position of the liner cooling air flow was altered by using a single- or double-wall liner design.

2. Numerical simulation

2.1 Field description and combustion conditions

Figure 1 shows a sector combustor (a 1/6 circumferentially divided donut-shaped full-annular combustor) and a combustion visualization view (a 1/18 sector combustor with a transparent quartz glass wall for visualization). The combustor design is RQL (Rich burn, Quick quench, Lean burn), which is one type of low-NO_x combustor design.

Figure 2 explains the concept of an RQL combustor. To avoid high-temperature zones where the equivalence ratio is near 1 and thermal NO_x is likely to be generated, an RQL combustor has two major combustion regions. One is the primary combustion region with a high equivalence ratio in the upstream region, and the other is the lean combustion region with a low equivalence ratio in the downstream region. The large amount of air entering from the dilution hole between the two regions rapidly dilutes and mixes with the combustion gas with a high equivalence ratio (fuel-rich combustion) generated in the primary combustion region to make a shift to lean combustion, thus suppressing NO_x generation.

Figure 3 shows the computational domain and the grids. The number of nodes is approximately 230000 and the number of elements is approximately 800000. The inflow boundary is set to fixed air flow conditions according to the test parameters, the outflow boundary is set to pressure boundary conditions, and the side wall boundary is set to periodic boundary conditions.

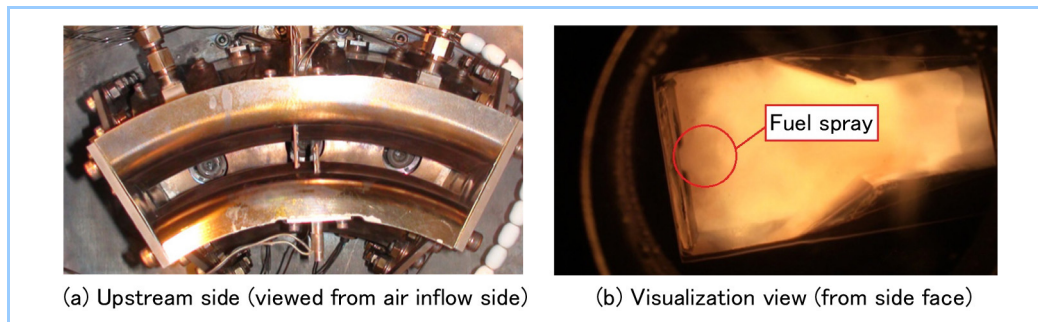


Figure 1 Sector combustor

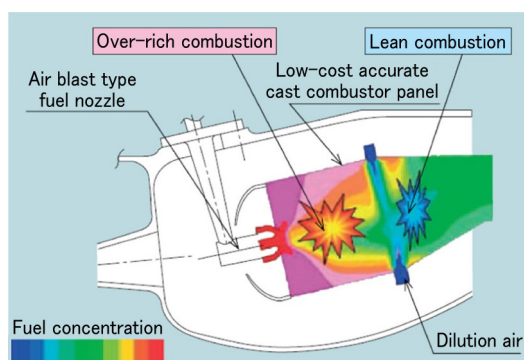


Figure 2 Schematic diagram of RQL combustor

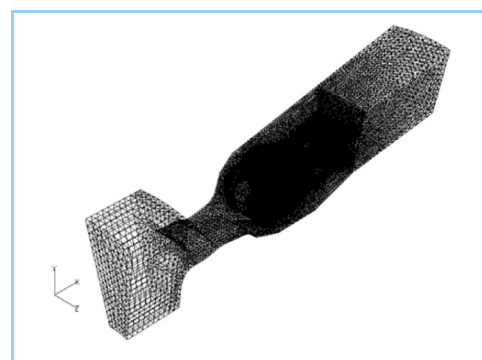


Figure 3 Computational domain and grids

The climb condition of an aircraft (equivalent to approximately 85% of the maximum load when taking off), where the amount of NO_x generation becomes most critical in terms of NO_x regulation and data have been acquired in the sector combustion test described above, was chosen for simulation. The three investigated designs are summarized in **Figure 4**. Dimension D in the figure represents the diameter of the dilution hole. CASE 1 is the base liner design. In CASE 2, the dilution flow balance between the outer liner and the inner liner was changed by increasing the

dilution hole size on the outer liner side and decreasing the dilution hole size on the inner liner side, while the total dilution hole area was kept constant. In CASE 3, the single-wall liner of the primary combustion region was changed to a double-wall liner to move the liner cooling air outlet location downstream of the primary combustion region.

The fuel spray shown in Figure 4 (inside the circle “Fuel spray”) is a simulation result. This looks similar to the real spray shown in the combustion visualization view of Figure 1 (inside the circle “Fuel spray”).

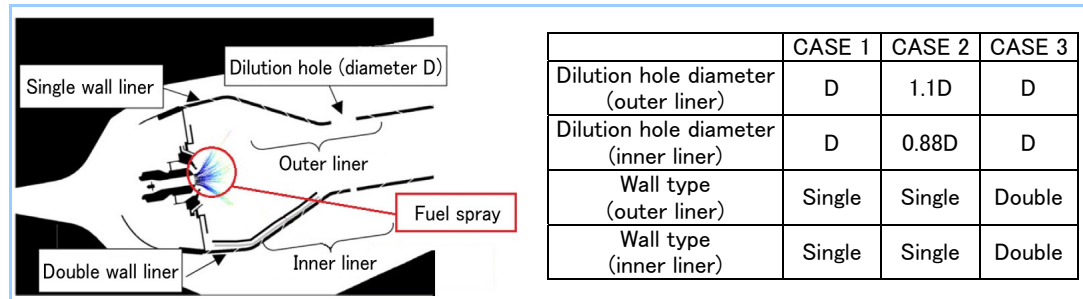


Figure 4 Analysis conditions

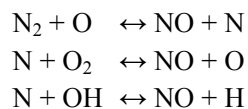
2.2 Numerical methods

STAR-CD Ver. 3.26 was used for simulation. The applied numerical methods are summarized below.

- Fuel : Dodecane $C_{12}H_{26}$ (simulation of JET-A fuel)
- Combustion model : Eddy Breakup model
- Droplet diameter distribution : Rosin-Rammler model
- Droplet breakup : Reitz-Diwakar model
- Chemical reaction equations (three-step general reaction)
 - $C_{12}H_{26} + 6O_2 \rightarrow 12CO + 13H_2$
 - $CO + 0.5O_2 \rightarrow CO_2$
 - $H_2 + 0.5O_2 \rightarrow H_2O$
- Convection term discretization scheme : MARS (Monotone Advection and Reconstruction Scheme)
- Simulation scheme : Three-dimensional compressible steady flow
- Turbulence model : Standard k- ϵ model

2.3 NO_x model

In this study, only nitrogen monoxide (NO) was examined as NO_x. NO generated in combustion can be roughly classified into two types: thermal NO generated directly from N₂ in the airflow for combustion and fuel NO generated from the nitrogen component in the fuel. In addition, thermal NO consists of Zeldovich NO, which follows the extended Zeldovich mechanism:



and prompt NO, which are generated from HCN, CN, etc. by the reaction between the N₂ in the airflow and the hydrocarbon in the fuel. However, only the former is considered to observe the tendency of NO generation in the combustor. The amount of Zeldovich NO generation was evaluated using quasi-steady approximation of the nitrogen component and the reaction rate constants of Baulch et al.⁽²⁾

NO calculation was conducted after completion of the steady calculation of the spray combustion flow field, as the NO concentration was small enough compared to the other combustion products and the reaction time scale was larger than that of hydrocarbon combustion, resulting in little effect on the spray combustion flow field. Specifically, the NO concentration distribution was obtained by acquiring the NO generation speed from the concentration of each chemical species in a steady state and solving the steady-state balance of generation, dissipation, and advection of NO in each cell.

3. Results and discussion

3.1 Features of spray combustion field in combustor

First, CASE 1, which represents the base conditions, is discussed as a representative case, and then the features of the spray combustion field in this study are described.

Figure 5 shows the distribution of the absolute velocity field obtained through this numerical simulation. In this figure, the four characteristic zones (A, B, C, and D) are shown with the added red solid arrows, which clearly indicate the flow tendencies. In the figure, the highest absolute velocity values can be seen in the lean combustion region (zone D) located downstream of the dilution hole, and the airflow from the dilution hole is quickly mixed in this region by the staggered arrangement of the dilution holes between the inner and the outer liner sides.

Although the magnitude of velocity in the vicinity of the fuel spray is also high, the flow spreads while forming a swirl flow and the velocity decreases quickly. In the primary combustion region, the recirculating flow, which contributes to flame stabilization, is formed in the center of the area located downstream of the fuel nozzle (zone A) and near the upstream liner wall surface (zone B). The main stream that leads to the downstream lean combustion region is a region along the liner wall surface (zone C).

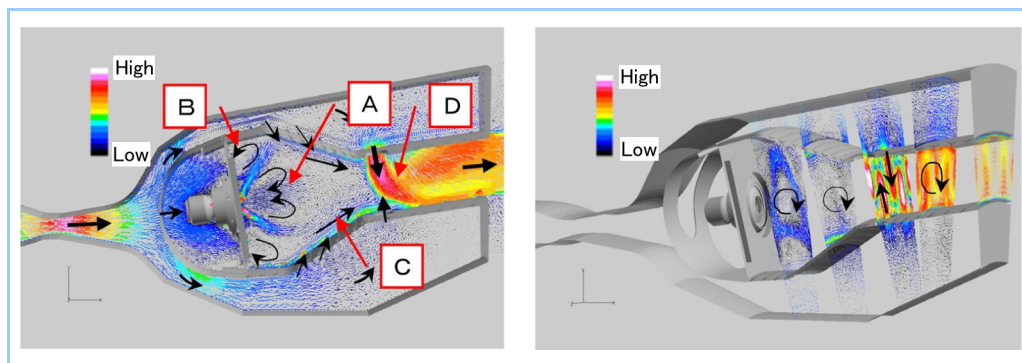


Figure 5 Velocity distribution (CASE 1)

Figures 6 – 9 show the cross-sectional distributions of fuel mass fraction, O_2 mass fraction, temperature, and NO_x (NO) mass fraction in the combustor, respectively, each obtained through this numerical simulation. Zones A – D in Figure 8 are in the same positions as those in Figure 5. These figures show the features of typical RQL combustors. Little O_2 is present in the vicinity of the fuel spray cone and in the center of the primary combustion region (zone A), which is a recirculating zone, because of excess fuel (equivalence ratio > 1). Therefore, NO_x generation is suppressed because of the lower temperature in this region. The high-temperature zones in the primary combustion region are limited to the upstream recirculating zone (zone B) where the fuel is lean and the near-liner-wall zone where the rich fuel is mixed with the airflow that cooled the liner (zone C). The NO_x concentration distribution (Figure 9) roughly corresponds to this temperature distribution (Figure 8).

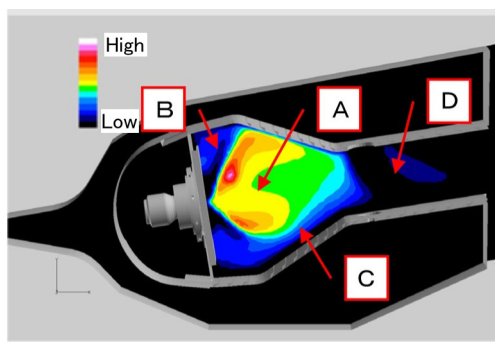


Figure 6 Fuel concentration distribution (CASE 1)

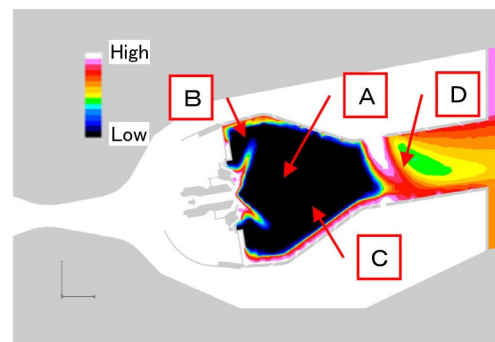


Figure 7 O_2 concentration distribution (CASE 1)

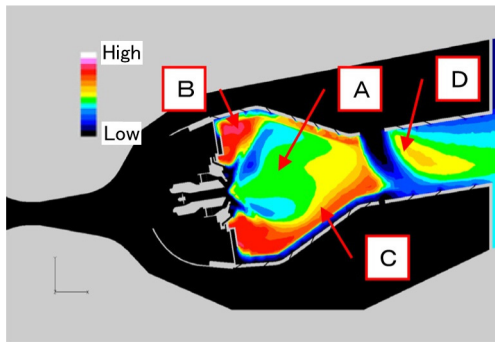


Figure 8 Temperature distribution (CASE 1)

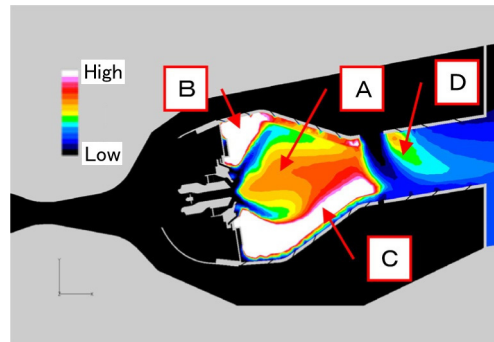


Figure 9 NOx concentration distribution (CASE 1)

NOx generated in the upstream region is transported downstream and diluted by the airflow from the dilution holes. Immediately after the dilution holes (zone D), the equivalence ratio becomes 1 locally, and the NOx concentration increases temporarily. However, subsequent mixing with air and the resulting dilution and temperature drop lead to a decrease in NOx concentration, ultimately reaching the combustor outlet. These results suggest that minimizing the NOx generation zone (high-temperature zone) as much as possible, in particular suppressing the mixing of the liner cooling airflow and the fuel rich flow in the main stream (zone C), is effective in avoiding the mass generation of high-temperature gas with an equivalence ratio of 1 and in decreasing NOx concentration (emission) at the combustor exit.

Figure 10 compares the distributions of the pressure normalized by the inlet pressure between the simulation and the experiment. The values obtained through the simulation correspond roughly to those obtained through experiment.

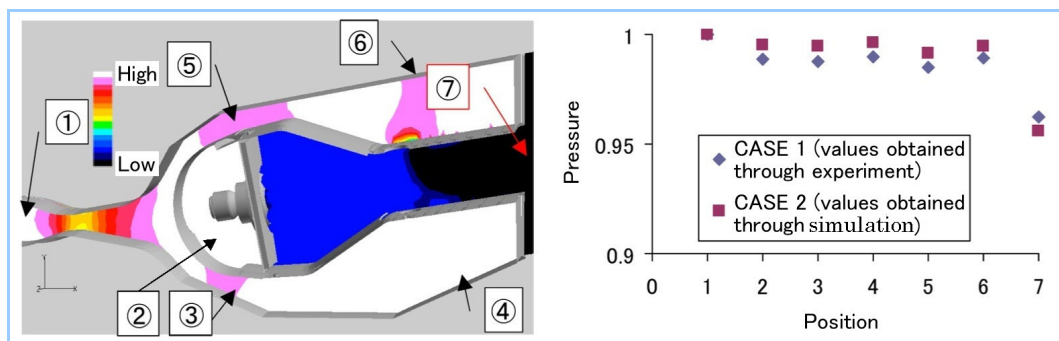


Figure 10 Pressure distribution (CASE 1)

3.2 Effects of dilution air balance and liner cooling air outflow position

Figures 11 – 14 show the cross-sectional distributions of temperature and NO mass fraction for CASE 2 and CASE 3 obtained through this numerical simulation. Compared to CASE 1 shown in Figures 8 and 9, CASE 2 has a similar temperature and NOx distribution in the primary combustion region but has a larger high-temperature region in the immediate downstream area of the larger dilution hole on the outer liner side and a higher NOx at the combustor exit.

The total amounts of dilution flow in CASE 1 and CASE 2 are the same, but the different dilution hole diameters between the inner and outer liners of CASE 2 are considered to cause entirely inhomogeneous mixing in the lean combustion region and make local high-temperature combustion regions with an equivalence ratio of ~ 1 , resulting in an increase in NOx.

On the other hand, the CASE 3 design resulted in a lower temperature at zone C and lower NOx concentrations at both the primary combustion region and the combustor exit compared to the other cases. This is because the temperature increase and NOx increase resulting from the mixing of the liner cooling air and the fuel rich primary combustion region occurring in CASE 1 and CASE 2 were suppressed in CASE 3. These observations indicate that a double-wall liner is very effective for NOx reduction.

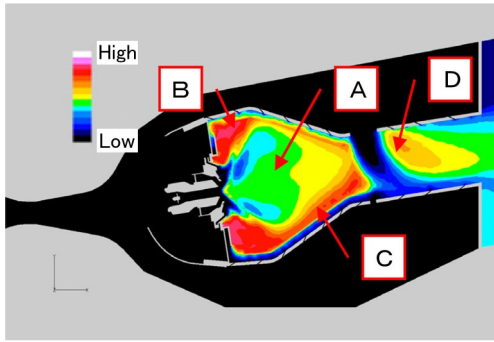


Figure 11 Temperature distribution (CASE 2)

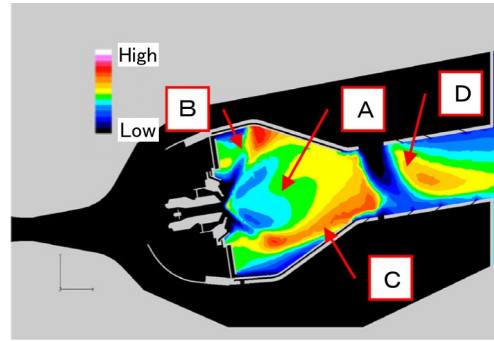


Figure 12 Temperature distribution (CASE 3)

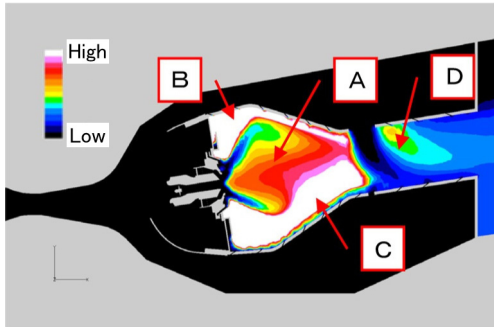


Figure 13 NOx concentration distribution (CASE 2)

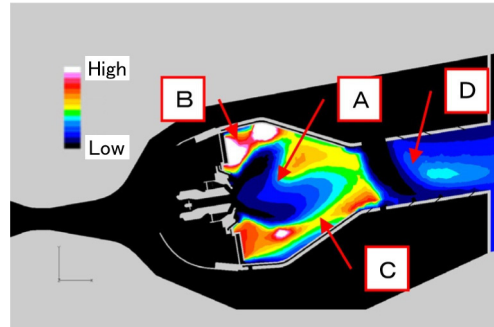


Figure 14 NOx concentration distribution (CASE 3)

Figure 15 compares the combustor exit NOx concentration (mass fraction) obtained through simulation and experiment for each case. In this figure, the NOx concentrations normalized by CASE 1 are shown for the simulation and the experiment. For both the simulation and the experiment, the NOx concentration increased in CASE 2 and decreased in CASE 3 compared to CASE 1. This indicates that RANS simulation can roughly predict the effects of liner cooling and dilution air flow balances. However, quantitatively, the level of NO obtained through the experiment is about three times greater than that in the simulation results. The improvement of the NOx model and the application of more accurate unsteady simulations, such as LES, will be necessary to achieve higher quantitative prediction accuracy.

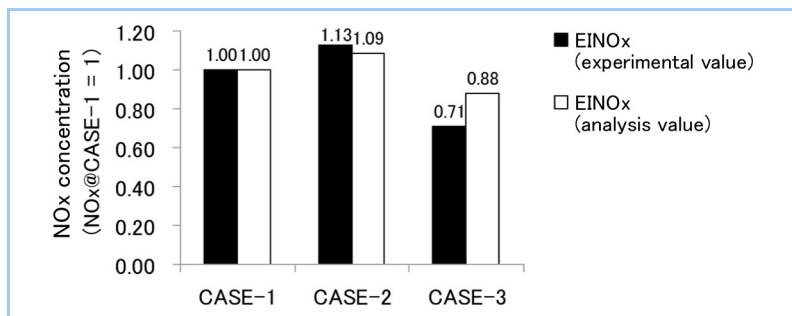


Figure 15 Comparison of NOx emission between prediction and experimental results

4. Conclusions

In this study, the effects of the dilution flow balance between the outer and inner liners of the aircraft gas turbine engine combustor and the difference between the single-wall liner and the double-wall liner on NOx performance were predicted using computational fluid dynamics (CFD), and experimental verification was performed. The results indicated that the use of CFD allows qualitative prediction of the flow inside the combustor and NOx performance, and that evenly balancing the dilution flow of the outer and inner liners and the use of a double-wall liner are effective for reduction of NOx. The results of the RANS simulation correspond qualitatively to those of the sector combustor tests, but the two differ quantitatively. This seems to be because the

accuracy of the NO_x model and the turbulence combustion model are insufficient. The application of simulation technology with greater accuracy, such as LES, is being studied to improve NO_x prediction.

Acknowledgements

The authors were instructed by Professor Satoru Komori and Associate Professor Ryoichi Kurose of Kyoto University. The combustion experiment data were obtained through tests carried out using the high-pressure combustion test facility at JAXA Chofu Aerospace Center (Chofu City, Tokyo, Japan). This research was supported by a research grant from NEDO (New Energy and Industrial Technology Development Organization). The authors would like express their gratitude to all those concerned.

References

1. Kurose, R., Akamatsu F., Experiments and Numerical Simulations of Spray Combustion, Journal of Combustion Society of Japan, Vol.50, pp.206-214 (2008).
2. Baulch, D.L. et al., Evaluated Kinetic Data for High Temperature Reactions, Butterworth (1973).